Antarctic Glacial Melt as a Driver of Recent Southern Ocean Climate Trends

Craig D. Rye[1*], John Marshall[2], Maxwell Kelley[3], Gary Russell[3], Larissa S Nazarenko[3], Yavor Kostov[4], Gavin A. Schmidt[3], James Hansen[1]

1. Earth Institute, Columbia University
2. Massachusetts Institute of Technology
3. Goddard Institute for Space Studies
4. University of Exeter

Corresponding author: craig.d.rye@gmail.com

Abstract

Recent trends in Southern Ocean (SO) climate – of surface cooling, freshening and sea-ice expansion – are not captured in historical simulations of state-of-the-art coupled climate models, suggesting that there may be a singular or multiple missing process(s). Here we demonstrate that the addition of plausible discharges of Antarctic meltwater in to a coupled climate model can produce a closer match to a wide range of climate trends found in observational records. We use an ensemble of simulations of the Goddard Institute for Space Studies Earth System Model (GISS-E2.1-G) to compute 'Climate Response Functions' (CRFs) for the addition of Antarctic meltwater. These imply a cooling and freshening of the SO, an expansion of winter sea ice and an increase in steric height, all consistent with observed trends since 1992. The CRF framework allows one to compare the efficacy of Antarctic meltwater as a driver of SO climate trends, relative to greenhouse gas and surface wind forcing. The meltwater CRFs presented here strongly suggest that interactive Antarctic ice melt must be included in models in order

to correctly hindcast the historical record and, by implication, make realistic future predictions.

1. Introduction

Observed and modelled decadal trends in Southern Ocean (SO) sea surface temperature (SST) and sea surface salinity (SSS) shown in Figure 1 reveal marked discrepancies: at the surface the models are ~0.12 ºC/dec warmer and ~0.03 PSU/dec saltier then observations during the period 1992-2014. Over the same period, Antarctic winter sea ice extent has increased by 2.4×10^5 km^2/dec (Zwally 2002; Comiso 2016) and Antarctic Subpolar Sea Surface Height (SSH) by around 1 cm/dec above the Southern Ocean rate (Rye et al., 2014). Hindcasting such trends in a consistent way is a difficult challenge and a notable deficiency of current coupled models used for climate change projections – see, e.g. Wang et al, (2014), Kostov et al, (2018).

Kostov et al., (2018) consider SO westerly wind forcing (as captured by the Southern Annular Mode, SAM, Marshall, 2003), and greenhouse gas (GHG) forcing as key drivers of the observed SO SST cooling. They examine the sensitivity of SO SST in Coupled Model Intercomparison Project (Phase 5) (CMIP5) models to observed trends in SAM and GHG forcing by diagnosing wind and GHG Climate Response Functions (CRFs) inferred from them. Linear convolution of the forcing with those CRFs implies an ensemble-mean warming of 0.04 ºC/ to GHG forcing and a cooling of 0.025 ºC/dec to SAM forcing. This implies a net (SAM+GHG) *warming* of 0.015 ºC/dec, across the 15 models considered, if GHG and winds were the only drivers. The observations (Figure 1), by contrast, reveal a *cooling* in excess of 0.05 ºC/dec. Here we argue that Antarctic glacial melt, although of uncertain magnitude, could induce such an additional cooling. Moreover, this cooling, and concomitant freshening, leads to sea-ice growth around Antarctica and sea-level rise in the Antarctic subpolar ocean all in broad agreement with the observational record.

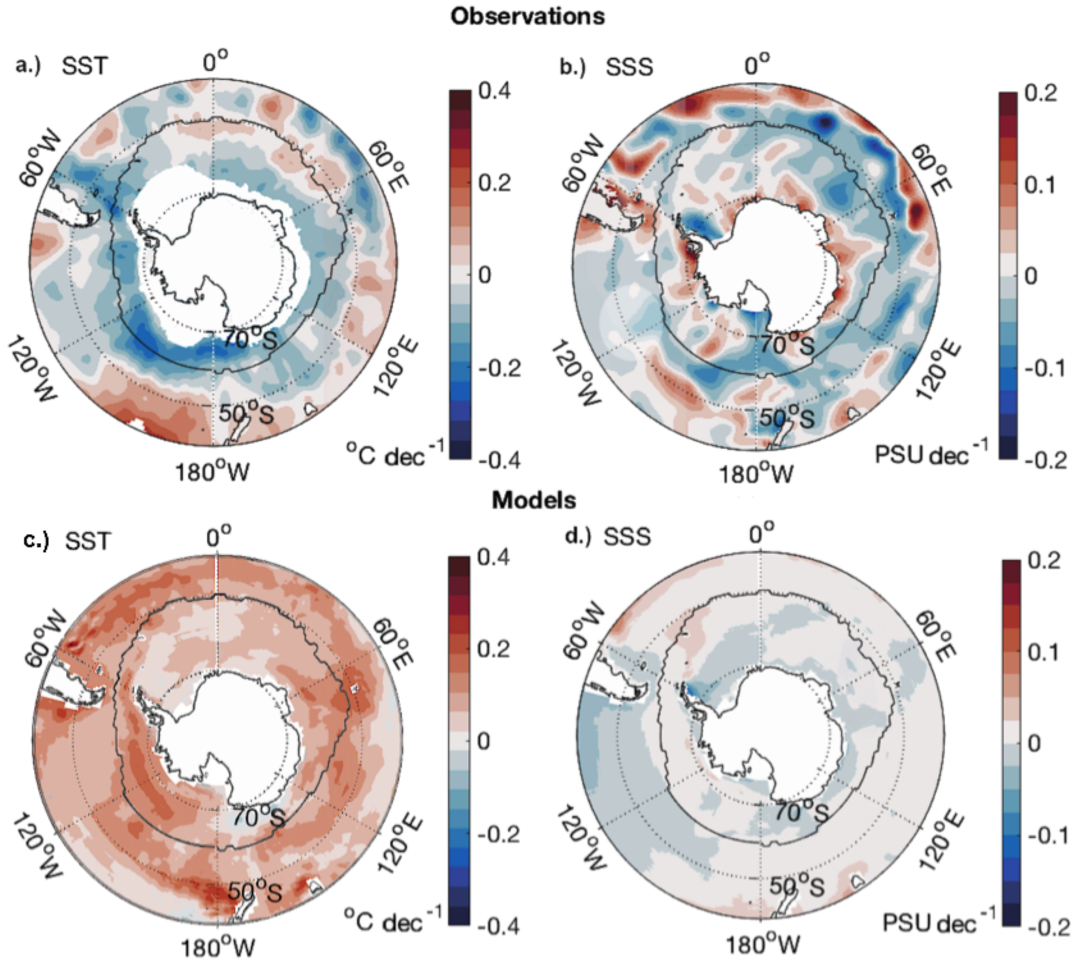

Figure 1| Simulated and Observed trends in Southern Ocean surface properties 1990-2014. a. Observed trend in SST (HadSST; Kennedy et al., 2014). b. Observed trend in SSS (CORA5; Cabanes et al., 2013). c. CMIP5 multi-model ensemble mean simulated trend in SST from the historical period 1990 to 2014. d. CMIP5 multi-model ensemble mean simulated trend in SSS. The black contour denotes the extent of winter sea ice maximum in observations.

CMIP5 earth system models do not represent the effect of Antarctic glacial melt. Observations, however, show that the grounded ice sheet melt rate around Antarctica has increased over recent decades to perhaps 250 Gt/yr in 2017 (IMBIE 2018). In addition to the grounded ice sheet, the thinning and retreat of floating ice shelves is thought to have contributed as much as 280 Gt/yr in recent years (2003-2015; Paolo 2015). Furthermore, other sources contribute large amounts of freshwater to the SO. For example, a series of large ice-shelf retreats not included in the above estimates could contribute an additional flux of perhaps 210 Gt/yr over the period 1988 and 2008 (Shepherd et al., 2010).

A number of studies have recently explored the response of the SO to perturbations in Antarctic meltwater in a variety of coupled and ocean-only models. For example, Rye et al., (2014), Fogwill et al., (2015), Hansen et al., (2016), Pauling et al (2016), Bronselaer et al., (2018) and Golledge et al., (2019). These suggest that the surface SO and subsurface Antarctic shelf sea cool and warm respectively in response to an increase in Antarctic meltwater. A number of studies have explored the response of Antarctic sea ice to an increase in Antarctic meltwater with rather variable results. For example, Bintangja et al 2013 and 2015 find that a glacial melt flux of around 180 Gt/yr is sufficient to reproduce the observed increase in sea ice between 1992 and 2015. In contrast, Pauling et al., 2016 suggests that a larger forcing of 3000 Gt/yr is required. Pauling et al (2017) find that an accelerating glacial melt flux of 45 Gt/yr/yr, up to a 4000 Gt/yr is sufficient to offset the decline in sea ice found in their model. Finally, Rye et al., (2014) highlights an anomalous trend in Antarctic Subpolar Sea Surface Height (SSH) and finds that a glacial melt rate of around 450 Gt/yr is sufficient to drive a steric increase consistent with observations.

Here we use a novel Climate Response Function (CRF) analysis to probe the role of Antarctic glacial melt in inducing recent climate trends in the SO, and its potency relative to other forcing such as GHG forcing and westerly wind trends. There is large uncertainty in the observed magnitude of meltwater flux; the CRF approach allows the response to any chosen meltwater time history to be inferred, provided the system response is linear. We conclude that glacial melt is likely an important missing component required to account for the magnitude and trend in all of the aforementioned climate signals and, in particular, it can account for the persistence and expansion of sea-ice around Antarctica in a warming world.

2. Response of a coupled climate model to Antarctic Glacial Melt

We utilise the Goddard Institute for Space Studies ModelE2.1-G earth system model, details and evaluation of which can be found in Supplementary Material and Doddridge et al (2019). The pre-industrial climatological state of the coupled model has an excellent climatology, as summarized in Figure 2. Figure 2a and 2c show close agreement between the observed and simulated zonal mean SO SST and the winter sea ice extent respectively. The zonal mean temperature in the Atmosphere and Ocean, as well as the zonal mean winds and currents (Figure 2b and d) are also encouragingly close to the observed climatology.

The response to a given scenario of Antarctic meltwater is examined using ensemble perturbation experiments. The pre-industrial state is perturbed by a 200 Gt/yr step-change increase in glacial meltwater; meltwater is distributed evenly around the continent, between the surface and 200 m depth, consistent with regions of ice-berg calving and kept constant in time. Experimental design is described further in Supplementary Material. The additional meltwater adds fresh, cold water (due to extraction of latent heat required to melt the ice) that is released in the upper 200 meters of the ocean water column (Schmidt et al 2014) in a spatially-uniform manner, over an area around Antarctica indicated by the light blue shading shown in Figure 2c. The perturbation experiments are run for 30 years. Twenty ensemble members are averaged to ensure that the signal is cleanly separated from internal variability. Additional experiments were conducted in which the meltwater anomaly was added regionally in either in the West Antarctic or East Antarctic; however, the placement of the anomaly within the Shelf Sea had negligible effect on the integrated SST response.

Linear Convolution Theory (LCT) (see, for example, Kostov et al., 2018) allows one to construct the response for any given meltwater scenario, to the extent that the response is linear. Our experiments show that the response is non-linear for forcing's that are an order of magnitude larger than the reference CRF experiment suggesting that contemporary climate change is in the linear regime.

The surface response of the model to a 200 Gt/yr step change in Antarctic glacial meltwater is shown in Figure 3. The meltwater induces a circumpolar band of cooling (0.03 ºC/dec) and freshening (0.004 PSU/dec) together with an expansion of the winter sea ice extent ($1.2x10^5$ km^2/dec compared to an observed trend of around $2x10^5$ km^2/dec; Comiso 2017). Cooling is concentrated around the northern extent of the winter sea ice. There is no trend under the sea ice where ice-ocean fluxes keep the water near its freezing point.

In the upper 500m of the water column one observes cooling and freshening between 70 and 20ºS. The upper 1000 m of the shelf waters become fresher and the intermediate depth shelf waters slightly saltier. Between 50 and 3000m depth, however, the response on the Antarctic margin is one of warming at depth. The combined surface freshening and deep warming on the Antarctic Shelf produces a steric increase in SSH of 0.3 cm/dec. The sign and magnitude of these responses are broadly consistent with observed trends over the past decades.

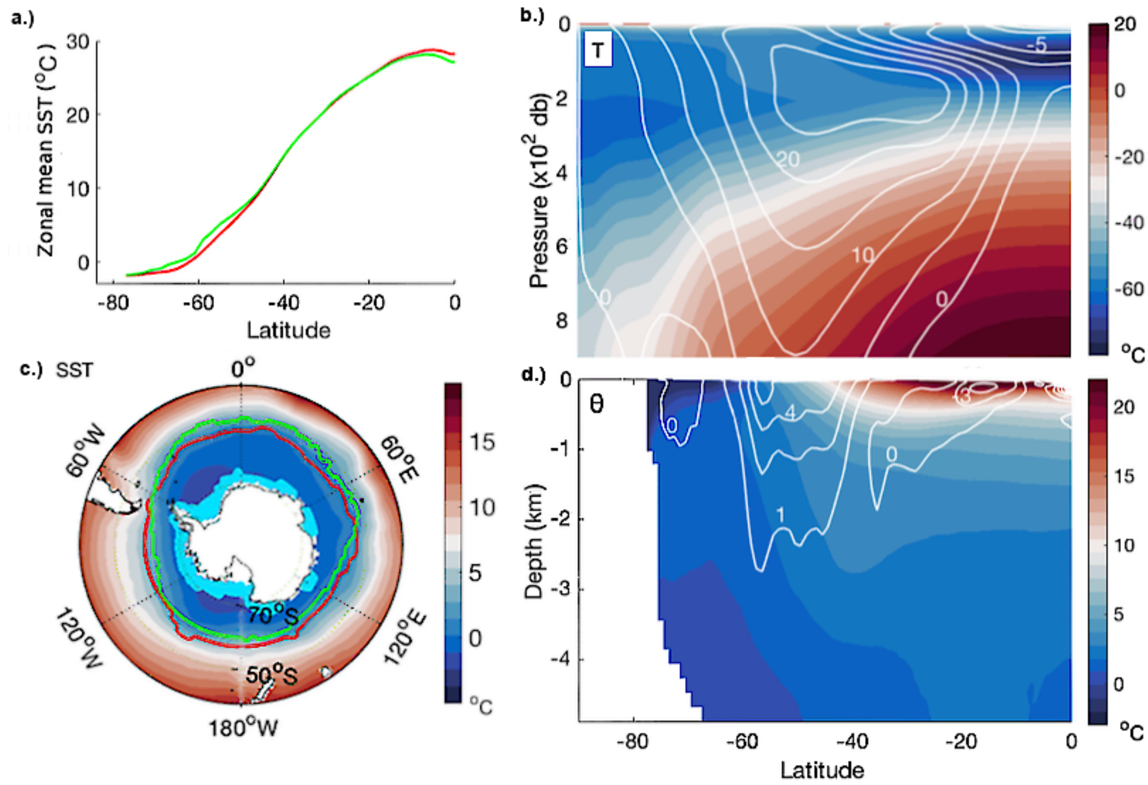

Figure 2| Southern Hemisphere Climatology of ModelE2.1-G. a. Zonal mean Southern Ocean SST in observations (green) and from the model (red). b. Modeled zonal mean atmospheric temperature. Contours denote the zonal mean zonal velocities (ms^{-1}). c. Plan view of SST in the coupled model. The winter sea ice extent is denoted by contours, from observations (green) and the model (red). The light blue region surrounding Antarctica denotes the area where glacial meltwater is fluxed into the ocean. d. Zonal mean potential temperature for the ocean. Contours denote zonal mean zonal velocities (cm s^{-1}).

3. Glacial Melt Response Functions: implications for understanding the historical record

The 200 Gt/yr perturbation experiment is now used to compute SST CRFs in response to glacial melt by integrating the time-evolution of the SST response over the circumpolar region, 55 to 70°S. It is shown in Figure 4a and should be compared to wind- and GHG-induced SST CRFs in Figs 4b and c, respectively, evaluated over the same area. The wind CRF from ModelE was obtained by computing lagged regressions between SAM and SST from a long control run (as described in Kostov et al, 2018) and – somewhat equivalently - by computing ozone-hole CRFs, which strongly project on to SAM (Doddridge et al., 2019). The GHG CRF of ModelE was computed by carrying instantaneous 2xCO2 experiments, a common method of assessing and comparing the response of climate models to GHG perturbations.

We see that in response to glacial melt, SST around Antarctica decays over the first twenty years to reach a new (cooler) equilibrium temperature after 30 years or so. As suggested by, for example, Rintoul (2001), fresh glacial melt is rapidly dispersed northwards in the wind-driven Ekman layer and carried eastwards in the swiftly flowing surface expression of the Antarctic Circumpolar Current. The surface becomes more stably stratified, the mixed layers slightly shallower and thus, because of the pronounced temperature inversion typical of waters adjacent to Antarctica, colder water is brought to the surface. This cooling

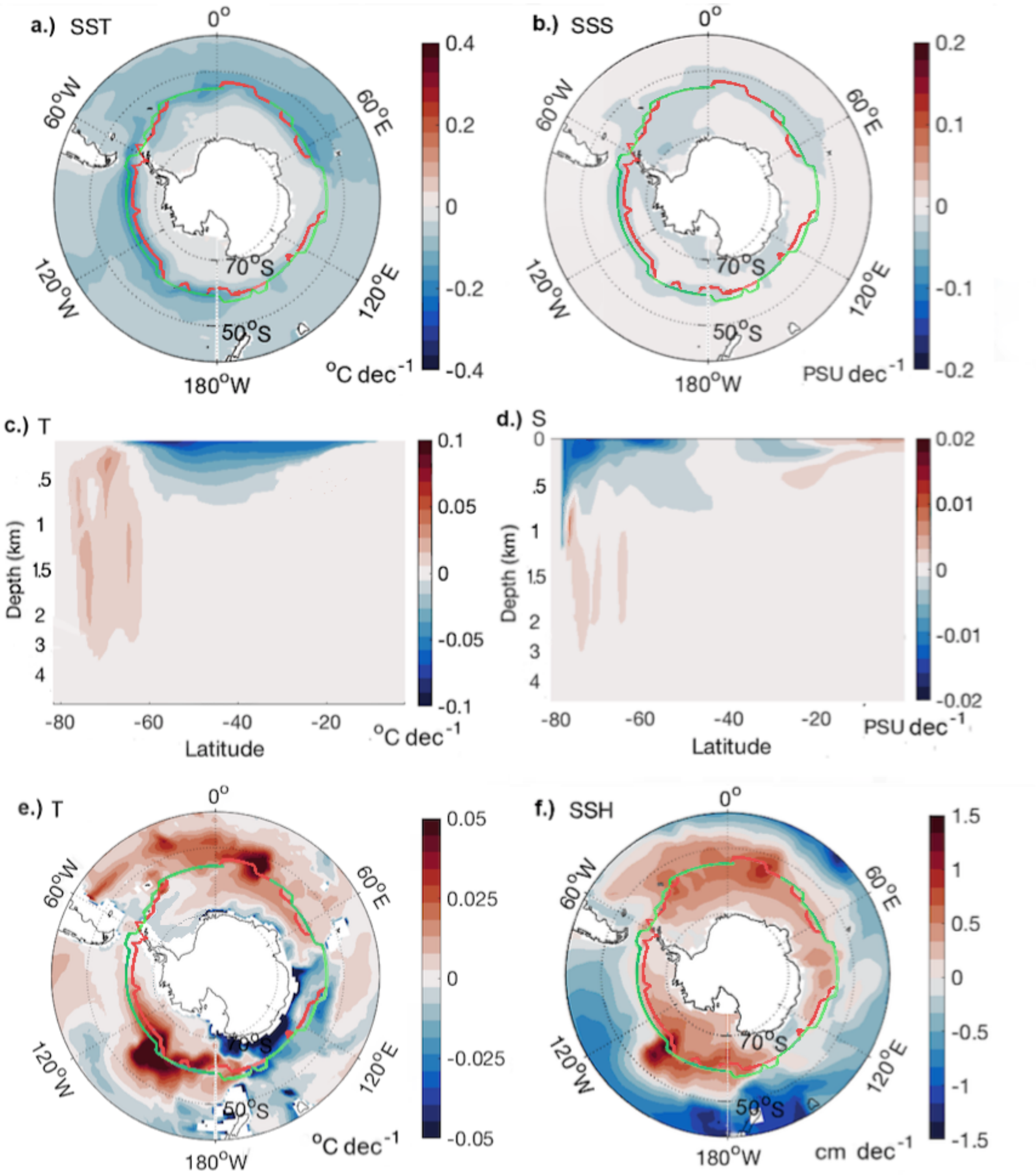

Figure 3| Modeled response to a 200 Gt yr^{-1} step change in glacial melt. Decadal trends calculated over 30 year model runs from a 20-member ensemble in (a) SST, (b) SSS (c) zonal-average potential temperature (d) zonal-average salinity (e) Interior temperature, averaged between 500 and 3000 m depth. (f) SSH. Red and Green contours denote the winter Sea Ice extent in the control run and after 30 years of perturbation experiment respectively.

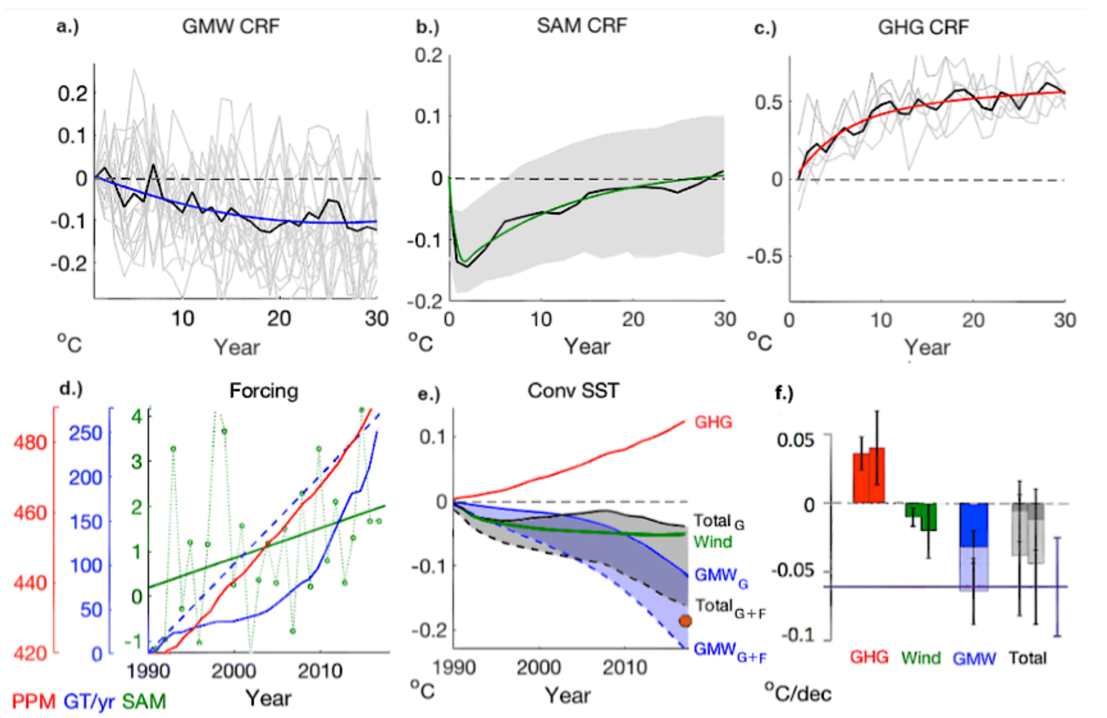

Figure 4| Linear convolution projections of Southern Ocean SST. ModelE Southern Ocean SST Climate Response Functions (CRFs) for: (a) 200 Gt/yr step change in Antarctic glacial melt, (b) a 1-standard deviation step-change in the Southern Annular mode (data provided by Doddridge (2019). Grey area: uncertainty estimate from the CMIP-5 multi-model spread. (c) a step-change doubling of CO2 forcing. In all plots the Grey lines indicate individual ensemble members and the black lines are ensemble means. Blue. Green and Red lines: Exponential fits to ensemble means. (d) Observed forcing histories for Green Houses Gases (GHG; Red line), Antarctic Glacial Melt Water (GMW; Blue lines) and Southern Annular Mode (SAM; Green line) provided by NOAA (Butler et al., 1999), IMBIE (IMBIE 2018), BAS (Marshall 2003). The GMW forcing history (Blue lines) is given for both grounded ice (solid line; GMW_G) and floating ice shelf (dashed line; GMW_F), where the floating ice shelf time history is assumed to be linear. (e) The convolution of CRFs (a-c) with forcing histories (d). Red line: GHGs. Green line: SAM (wind). Blue full line: GMW_G from the grounded ice sheet. Blue dashed line: GMW_{G+F} from the grounded ice sheet and floating ice shelves. Shaded blue area: region between lower and upper bound estimates of glacial melt forcing. Full black line: the combined response, $Total_G$. Dashed line: the combined response, $Total_{G+F}$, including the additional GMW associated with the melt of floating ice shelves. The orange dot marks the observed Southern Ocean SST cooling. (f) Summary of Southern Ocean SST trends per decade. Red bars: GHG. Green bars: SAM (Wind). Blue bar: GMW. Grey bars: Combined forcing. For GHG, Wind and Total, the left-side bar shows convolution results for ModelE and the right-side bar shows results for the CMIP-5 multi-model mean derived from Kostov et al., (2018) and Doddridge et al., (2019). For GMW and Total, the full bars denote convolutions for the time histories of grounded Antarctic meltwater; the shaded bars denote convolutions for the combined time history of grounded ice and floating ice shelves. The purple line marks the observed Southern Ocean cooling. Black whiskers show uncertainty estimates.

signature is very different from, and should be contrasted to, that induced by a step-change in the winds, shown in Fig.4b. This exhibits a 2-timescale response discussed at length in Marshall et al., (2014), Ferreira et al., (2015), and Doddridge et al., (2019): a rapid, Ekman-driven initial cooling followed by a (much) slower warming tendency due to the upwelling of warm water from below. The GHG CRF is shown in Fig.4c and is a mirror-image of the glacial melt response, but with the familiar warming signal rising toward an equilibrium on timescales of 30 years.

Having computed CRFs for these three key drivers of Antarctic climate change, we can convolve them (see Equation 1 of Supplementary Material) with historical estimates of trends in glacial melt, SAM and GHG forcing (shown in Fig.4d) to assess their relative importance in explaining the historical record. Results of such convolutions are given in Fig. 4e and f. GHG forcing produces an almost linear trend in SO SST of around 0.04ºC/dec. The recent trend in SAM produces a small SO SST cooling of around 0.02ºC/dec. Finally the grounded ice Glacial Melt Water (GMW) CRF produces a relatively large cooling of around 0.04 ºC/dec. The GMW response is computed from the recent time history of melt associated with an accelerated melting of the grounded ice-sheet between 2005 and present. The combined response of GHG, SAM and grounded GMW leads to a slight overall cooling that offsets the GHG-driven warming but suggests no clear cooling trend between 1990 and present.

Following Rye et al., 2014 and Paolo et al., 2015 it is reasonable to increase the meltwater flux in projections to account for the additional 280 Gt/yr meltwater produced by floating ice shelves. Although of rather uncertain magnitude, this might be considered a lower bound as it neglects the additional melt associated with the break up of ice shelves (Shepherd et al., 2010). If floating ice shelf melt is included and used to drive our linear convolution, the combination of total Antarctic meltwater (now reaching 530 Gt/yr in recent years), GHG forcing and an upward trend in SAM leads to a net cooling of SST of around 0.05 ºC/dec, in closer agreement with observations. This is summarised in (Figure 4f).

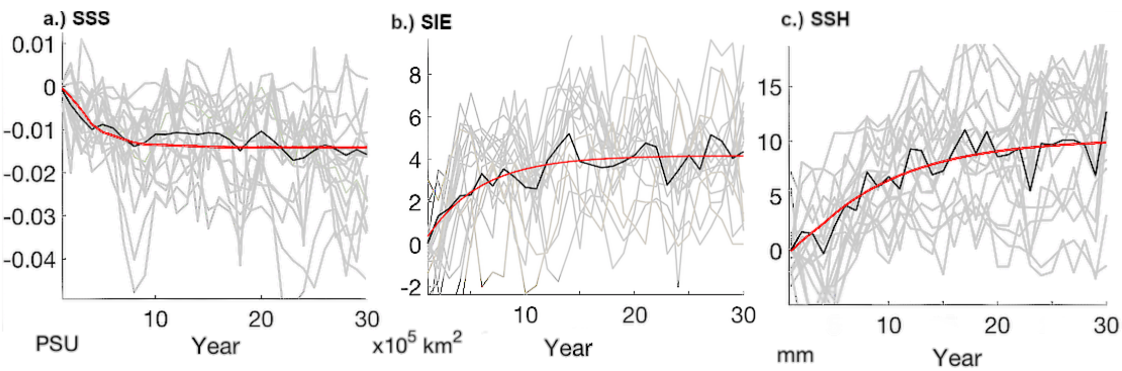

Figure 5| Southern Ocean Climate Response Functions. ModelE CRFs for a 200 Gt/yr step change in Antarctic glacial melt. Grey lines: individual ensemble members. Black line: Ensemble mean. Red lines: Exponential or linear fit to ensemble mean. (a) Sea Surface Salinity averaged over 55 to 70 S. (b) Winter Sea Ice Extent. (c) Antarctic Subpolar Sea Sea Surface Height averaged between the continent and 70 S.

The 200 Gt/yr perturbation experiment can be used to compute CRFs for SSS, Sea-Ice Extent (SIE) and SSH by integrating those quantities over the circumpolar region and plotting them as a function of time. They are shown in Figs. 5a-c respectively. Here, meltwater drives a rapid decline in SST and SSS as well as an increase in SIE. The majority of the surface adjustment occurs in the initial 10 years. The response of the SSH is linear and shows the least spread between ensembles. The response of the abyssal temperature is relatively slow. As expected, the deep temperature and SSH adjustment is far from equilibrium after 30 years. The response of SSS, SIE, and SSH is in broad agreement with observations (see, e.g. Cabanes et al., 2013, Rayner 2003, Rye et al., 2014). We thus see that increasing the melt rate to 530 Gt/yr, by including meltwater from floating ice shelves, improves agreement observations.

Discussion and Conclusions

It is difficult to account for observed recent decadal trends in SST and sea-ice extent if one only invokes GHG and wind forcing (whether induced by natural variability or ozone forcing). Most, if not all, coupled climate models are unable to capture these trends suggesting that a process which is currently missing in our models is likely at work. Here we have shown that including meltwater associated with grounded ice in one particular model – GISS ModelE – has a significant impact on the SO properties and may account for 40% or so of the observed cooling. Moreover, if one also includes the effect of rather uncertain meltwater rates from floating ice shelves, Antarctic glacial meltwater could account for all of the observed cooling. That said, there is a large uncertainty in the current rate and future projections of Antarctic meltwater flux and, moreover, a large spread in the response of models to a meltwater pulse. This highlights the importance of quantifying the rates of glacial melt and improving the representation of those processes that govern the response of the polar climate to such perturbations.

Introduction of glacial meltwater simultaneously improves multiple SO trends consistent with observations (particularly in SST, SIE and SSH). Moreover, the response of the SO climate in models is broadly consistent across studies. For example, glacial melt driven SO SST cooling is found by Stoufer et al., (2006), Bintanja et al., (2013), Hansen et al., (2016), Bronselaer et al., (2018), Park and Latif (2018) and Golledge et al., (2019); glacial melt driven SO SIE expansion is found by Aiken and England (2008), Bintanja (2013), Swart and Fyfe (2013), Bintangja et al., (2015), Pauling et al., (2016) and Merino et al., (2018); finally glacial melt driven Subpolar Sea SSH anomaly is found by Rye et al., (2014) and Merino et al., (2018). It is notable that the above modelling studies do not emphasize melt water flux associated with floating ice shelves and from the large ice shelve retreats discussed by Paolo (2015) and Shepherd et al., (2010) respectively.

Although the sense of climate trends induced by Antarctic glacial melt appear to be broadly consistent across models, there is a wide spread in the magnitude of the response, particularly in respect of sea ice. For example, the work of Bintanja (2013) found that an Antarctic mass flux of 180 Gt/yr is sufficient to produce a small positive trend in sea ice, consistent with observations. In contrast Pauling et al., (2016), argue that even larger freshwater forcings of e.g. 2000 Gt/yr are insufficient to account for the recent trend in sea ice expansion. The addition of 250 Gt/yr meltwater to ModelE2.1 produces an increase in sea ice that accounts for roughly half of the observed trend. The addition of around 530 Gt/yr to ModelE2.1 can account for most of the observed trend. Clearly, much more work is required to explore the causes of these inter-model differences.

Finally, it should be said that in addition to meltwater, there are multiple other SO freshwater sources that complicate our discussion. For example, changes in precipitation are difficult to account for. Multi-model projections suggest that there is no significant trend in SO precipitation over recent decades (Bromwich 2011); however, the freshwater perturbation associated with a standard deviation in precipitation is substantially larger than that currently produced by the grounded ice sheet. Purich (2018) considers the response of the SO to a precipitation anomaly and finds broadly consistent results, in which additional precipitation leads to surface circumpolar cooling and freshening. Furthermore, wind driven sea ice variability (Holland et al., 2012) also creates salinity perturbations that are an order of magnitude larger than those resulting from grounded ice sheets (Abernathey et al, 2016). That said, earth system models aim to capture changes in precipitation, which, unlike perhaps glaciers, cannot be considered to be ‘external’ to the system on our timescales of interest.

We conclude that the “missing process” implied by the mismatch seen in Fig. 1 is very likely related to Antarctic glacial melt. The match to multiple SO trends in disparate quantities, none of which appear in the CMIP5 ensemble, is strong evidence that this process is not only active, but dominant, and thus needs to be incorporated into future projections. Constraining the exact magnitude of the melt water rate is challenging but we judge that a range of between 200 Gt/yr and 800 Gt/yr of GMW is most consistent with observations.

References

Abernathey, R.P., Cerovecki, I., Holland, P.R., Newsom, E., Mazloff, M. and Talley, L.D., 2016. Water-mass transformation by sea ice in the upper branch of the Southern Ocean overturning. *Nature Geoscience*, *9*(8), p.596.

Aiken, C.M. and England, M.H., 2008. Sensitivity of the present-day climate to freshwater forcing associated with Antarctic sea ice loss. *Journal of Climate*, *21*(15), pp.3936-3946.

Bronselaer, B., Winton, M., Griffies, S.M., Hurlin, W.J., Rodgers, K.B., Sergienko, O.V., Stouffer, R.J. and Russell, J.L., 2018. Change in future climate due to Antarctic meltwater. *Nature*, *564*(7734), p.53.

Bromwich, D.H., Nicolas, J.P. and Monaghan, A.J., 2011. An assessment of precipitation changes over Antarctica and the Southern Ocean since 1989 in contemporary global reanalyses. *Journal of Climate*, *24*(16), pp.4189-4209.

Butler, J.H., Battle, M., Bender, M., Montzka, S.A., Clarke, A.D., Saltzman, E.S., Sucher, C., Severinghaus, J. and Elkins, J.W., 1999. A twentieth century record of atmospheric halocarbons in polar firn air. *Nature*, *399*(6738), pp.749-755.

Bintanja, R., Van Oldenborgh, G.J., Drijfhout, S.S., Wouters, B. and Katsman, C.A., 2013. Important role for ocean warming and increased ice-shelf melt in Antarctic sea-ice expansion. *Nature Geoscience*, *6*(5), p.376.

Bintanja, R., Van Oldenborgh, G.J. and Katsman, C.A., 2015. The effect of increased fresh water from Antarctic ice shelves on future trends in Antarctic sea ice. *Annals of Glaciology*, *56*(69), pp.120-126.

Bitz, C.M. and Lipscomb, W.H., 1999. An energy‐conserving thermodynamic model of sea ice. *Journal of Geophysical Research: Oceans*, *104*(C7), pp.15669-15677.

Cabanes, C., Grouazel, A., Schuckmann, K.V., Hamon, M., Turpin, V., Coatanoan, C., Paris, F., Guinehut, S., Boone, C., Ferry, N. and Boyer Montégut, C.D., 2013. The CORA dataset: validation and diagnostics of in-situ ocean temperature and salinity measurements. *Ocean Science*, *9*(1), pp.1-18.

Chen, C., Liu, H. and Beardsley, R.C., 2003. An unstructured grid, finite-volume, three-dimensional, primitive equations ocean model: application to coastal ocean and estuaries. *Journal of atmospheric and oceanic technology*, *20*(1), pp.159-186.

Comiso, J.C., Gersten, R.A., Stock, L.V., Turner, J., Perez, G.J. and Cho, K., 2017. Positive trend in the Antarctic sea ice cover and associated changes in surface temperature. *Journal of Climate*, *30*(6), pp.2251-2267.

DeConto, R.M. and Pollard, D., 2016. Contribution of Antarctica to past and future sea-level rise. *Nature*, *531*(7596), p.591.

Doddridge, E.W., Marshall, J., Song, H., Campin, J.M., Kelley, M. and Nazarenko, L., 2019. Eddy Compensation Dampens Southern Ocean Sea Surface Temperature Response to Westerly Wind Trends. *Geophysical Research Letters*, *46*(8), pp.4365-4377

Ferreira, D., Marshall, J., Bitz, C.M., Solomon, S. and Plumb, A., 2015. Antarctic Ocean and sea ice response to ozone depletion: A two-time-scale problem. *Journal of Climate*, *28*(3), pp.1206-1226

Fogwill, C.J., Phipps, S.J., Turney, C.S.M. and Golledge, N.R., 2015. Sensitivity of the Southern Ocean to enhanced regional Antarctic ice sheet meltwater input. *Earth's Future*, *3*(10), pp.317-329.

Gent, P.R. and McWilliams, J.C., 1996. Eliassen–Palm fluxes and the momentum equation in non-eddy-resolving ocean circulation models. *Journal of Physical Oceanography*, *26*(11), pp.2539-2546. ?

Golledge, N.R., Keller, E.D., Gomez, N., Naughten, K.A., Bernales, J., Trusel, L.D. and Edwards, T.L., 2019. Global environmental consequences of twenty-first-century ice-sheet melt. *Nature*, *566*(7742), p.65.

Griffies, S.M., 1998. The Gent–McWilliams skew flux. *Journal of Physical Oceanography*, *28*(5), pp.831-841.

Hansen, J., Sato, M., Hearty, P., Ruedy, R., Kelley, M., Masson-Delmotte, V., Russell, G., Tselioudis, G., Cao, J., Rignot, E. and Velicogna, I., 2016. Ice melt, sea level rise and superstorms: evidence from paleoclimate data, climate modeling, and modern observations that 2 C global warming could be dangerous. *Atmospheric Chemistry and Physics*, *16*(6), pp.3761-3812.

IMBIE 2018 Shepherd, A., Ivins, E., Rignot, E., Smith, B., Van Den Broeke, M., Velicogna, I., Whitehouse, P., Briggs, K., Joughin, I., Krinner, G. and Nowicki, S., 2018. Mass balance of the Antarctic Ice Sheet from 1992 to 2017. *Nature*, *558*, pp.219-222.

Kostov, Y., Ferreira, D., Armour, K.C. and Marshall, J., 2018. Contributions of greenhouse gas forcing and the southern annular mode to historical southern ocean surface temperature trends. *Geophysical Research Letters*, *45*(2), pp.1086-1097.

Lin, X., Zhai, X., Wang, Z. and Munday, D.R., 2018. Mean, variability, and trend of Southern Ocean wind stress: role of wind fluctuations. *Journal of Climate*, *31*(9), pp.3557-3573.

Large, W.G. and Gent, P.R., 1999. Validation of vertical mixing in an equatorial ocean model using large eddy simulations and observations. *Journal of Physical Oceanography*, *29*(3), pp.449-464.

Marshall, G.J., 2003. Trends in the Southern Annular Mode from observations and reanalyses. *Journal of Climate*, *16*(24), pp.4134-4143.

Marshall, G.J., 2003. Trends in the Southern Annular Mode from observations and reanalyses. *Journal of Climate*, *16*(24), pp.4134-4143.

Marshall, J., Armour, K.C., Scott, J.R., Kostov, Y., Hausmann, U., Ferreira, D., Shepherd, T.G. and Bitz, C.M., 2014. The ocean's role in polar climate change: asymmetric Arctic and

Antarctic responses to greenhouse gas and ozone forcing. *Philosophical Transactions of the Royal Society A: Mathematical, Physical and Engineering Sciences*, *372*(2019), p.20130040.

Merino, N., Jourdain, N.C., Le Sommer, J., Goosse, H., Mathiot, P. and Durand, G., 2018. Impact of increasing antarctic glacial freshwater release on regional sea-ice cover in the Southern Ocean. *Ocean Modelling*, *121*, pp.76-89.

Park, W. and Latif, M., 2018. Ensemble global warming simulations with idealized Antarctic meltwater input. *Climate Dynamics*, pp.1-17.

Paolo, F.S., Fricker, H.A. and Padman, L., 2015. Volume loss from Antarctic ice shelves is accelerating. *Science*, *348*(6232), pp.327-331.

Pauling, A.G., Bitz, C.M., Smith, I.J. and Langhorne, P.J., 2016. The response of the Southern Ocean and Antarctic sea ice to freshwater from ice shelves in an Earth system model. *Journal of Climate*, *29*(5), pp.1655-1672.

Purkey, S.G. and Johnson, G.C., 2013. Antarctic Bottom Water warming and freshening: Contributions to sea level rise, ocean freshwater budgets, and global heat gain. *Journal of Climate*, *26*(16), pp.6105-6122.

Purich, A., England, M.H., Cai, W., Sullivan, A. and Durack, P.J., 2018. Impacts of broad-scale surface freshening of the Southern Ocean in a coupled climate model. *Journal of Climate*, *31*(7), pp.2613-2632.

Rayner, N. A.; Parker, D. E.; Horton, E. B.; Folland, C. K.; Alexander, L. V.; Rowell, D. P.; Kent, E. C.; Kaplan, A. (2003) Global analyses of sea surface temperature, sea ice, and night marine air temperature since the late nineteenth century, J. Geophys. Res., Vol. 108, No. D14, 4407 10.1029/2002JD002670

Russell, G.L., Miller, J.R. and Rind, D., 1995. A coupled atmosphere‐ocean model for transient climate change studies. *Atmosphere-ocean*, *33*(4), pp.683-730.

Russell, G.L., Miller, J.R., Rind, D., Ruedy, R.A., Schmidt, G.A. and Sheth, S., 2000. Comparison of model and observed regional temperature changes during the past 40 years. *Journal of Geophysical Research: Atmospheres*, *105*(D11), pp.14891-14898.

Rye, C.D., Garabato, A.C.N., Holland, P.R., Meredith, M.P., Nurser, A.G., Hughes, C.W., Coward, A.C. and Webb, D.J., 2014. Rapid sea-level rise along the Antarctic margins in response to increased glacial discharge. *Nature Geoscience*, *7*(10), p.732.

Shepherd, A. et al. Recent loss of floating ice and the consequent sea level contribution. Geophys. Res. Lett. 37, L13503 (2010).

Schmidt, G.A., Ruedy, R., Hansen, J.E., Aleinov, I., Bell, N., Bauer, M., Bauer, S., Cairns, B., Canuto, V., Cheng, Y. and Del Genio, A., 2006. Present-day atmospheric simulations using GISS ModelE: Comparison to in situ, satellite, and reanalysis data. *Journal of Climate*, *19*(2), pp.153-192.

Schmidt, G.A., Kelley, M., Nazarenko, L., Ruedy, R., Russell, G.L., Aleinov, I., Bauer, M., Bauer, S.E., Bhat, M.K., Bleck, R. and Canuto, V., 2014. Configuration and assessment of the GISS ModelE2 contributions to the CMIP5 archive. *Journal of Advances in Modeling Earth Systems*, *6*(1), pp.141-184.

Stouffer, R.J., Seidov, D. and Haupt, B.J., 2007. Climate response to external sources of freshwater: North Atlantic versus the Southern Ocean. *Journal of Climate*, *20*(3), pp.436-448.

Visbeck, M., Marshall, J., Haine, T. and Spall, M., 1997. Specification of eddy transfer coefficients in coarse-resolution ocean circulation models. *Journal of Physical Oceanography*, *27*(3), pp.381-402.

Wang, C., Zhang, L., Lee, S.K., Wu, L. and Mechoso, C.R., 2014. A global perspective on CMIP5 climate model biases. *Nature Climate Change*, *4*(3), p.201.

Yang, H., Liu, Q., Liu, Z., Wang, D. and Liu, X., 2002. A general circulation model study of the dynamics of the upper ocean circulation of the South China Sea. *Journal of Geophysical Research: Oceans*, *107*(C7).

Zwally, H.J., Comiso, J.C., Parkinson, C.L., Cavalieri, D.J. and Gloersen, P., 2002. Variability of Antarctic sea ice 1979–1998. *Journal of Geophysical Research: Oceans*, *107*(C5), pp.9-1.

Zhang, J. and Rothrock, D., 2000. Modeling Arctic sea ice with an efficient plastic solution. *Journal of Geophysical Research: Oceans*, *105*(C2), pp.3325-3338.

Supplementary Material

The Model

We use the NASA Goddard Institute for Space Studies (GISS) earth system model, ModelE. This configuration integrates Atmosphere, Ocean, Land and Cryosphere components (Hansen 1983; Schmidt et al., 2006; Schmidt et al., 2014). The Atmosphere comprises of 40 vertical levels with a horizontal resolution of 2^{o} x 2.5^{o}. It uses an Arakawa-B grid and a sigma vertical coordinate extending to 0.1 hPa. The atmosphere dynamical core, mixing, and boundary layer code are described by Schmidt et al., (2006). The Ocean has 40 vertical levels with 1^{o} horizontal resolution. It is a non-Boussinesq, mass conserving free surface model (Russell et al, 1995; Russell et al, 2000; Liu et al 2002; Liu et al., 2003). Ocean dynamics are based on a modified Arakawa C-grid scheme. Vertical mixing uses the KPP scheme (Large et al., 1996). Mesoscale eddies and isopycnal diffusion are parameterised by the Gent and McWilliams (1996) scheme with variable coefficients (Visbeck et al, 1997; Griffies 1998). The ModelE sea ice model consists of two mass layers and four thermal layers. Salinity and tracers are calculated on mass layers. Sea ice dynamics utilises the viscous-plastic formulation of Zhang and Rothrock (2000) and the brine-pocket thermodynamics of Bitz and Lipscomb (1999).

The ModelE ice-sheet model is coupled to the ocean through an idealised representation of melting ice-bergs, referred to as the implicit ice-berg array. The standard ice-sheet model is not dynamic and acts to maintain constant ice-sheet mass; excess precipitation onto the Antarctic continent is collected into the implicit ice-berg array and released into the ocean over a 10-year period. The ice-berg array distributes meltwater evenly as defined by the mask shown in figure 2. The standard ModelE ice-berg mask follows observations of ice berg calving (Tournadre et al., 2016). Meltwater is distributed evenly in the upper 200 meters. The ice-berg array has climatological annual flux of around 1800 Gt/yr, consistent with observations.

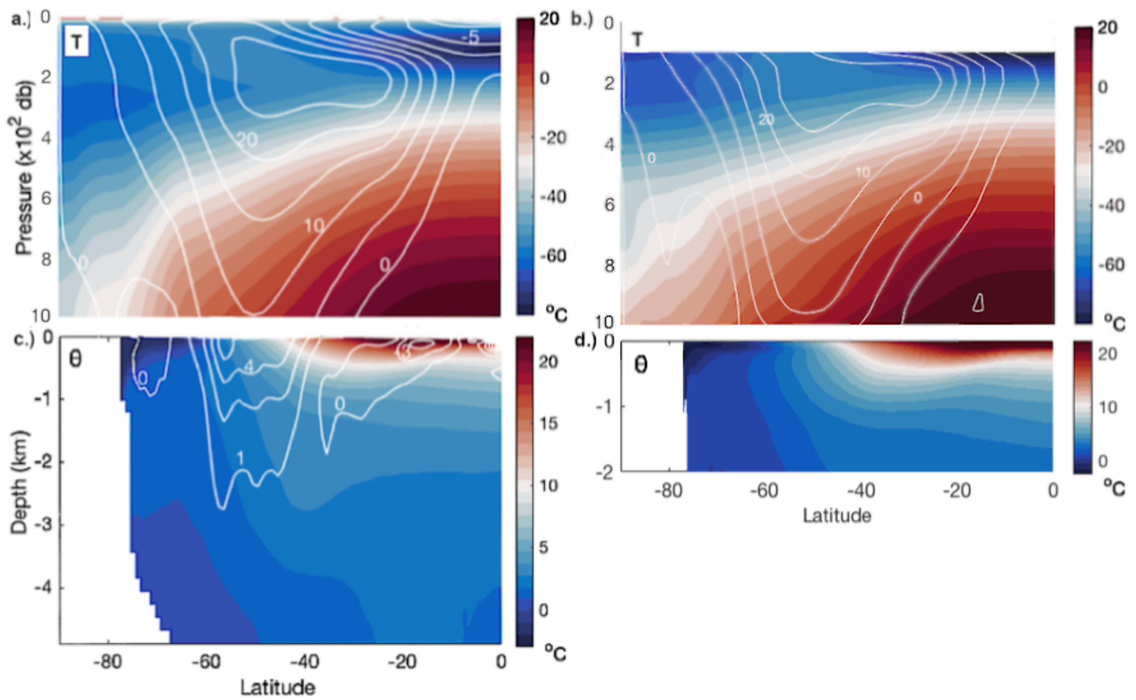

Figure S1| Southern Hemisphere Climatology of ModelE2.1-G. a. ModelE zonal mean atmospheric temperature. Contours denote the zonal mean zonal velocities (ms^{-1}). b. Era-Interim reanalysis zonal mean atmospheric temperature 1990-2000. Contours denote the zonal mean zonal velocities (ms^{-1}). c. ModelE zonal mean potential temperature for the ocean. Contours denote zonal mean zonal velocities ($cm\ s^{-1}$) (Era-Interim; Dee et al., 2011) .d. Argo ocean observed zonal mean potential temperature 1990-2000 (CORA5; Cabanes et al., 2013).

Experiment design

The model control run, with constant pre-industrial greenhouse gases and aerosols, is integrated for 500 to 700 years to reach near-equilibrium. Every 10 years along this state, an ensemble member experiment is initiated. In each experiment, an anomalous glacial meltwater flux is applied as an addition of mass and subtraction of heat energy (3.34 kJ kg^{-1}) to the ModelE implicit ice-berg array. The anomalous glacial meltwater is added in addition to the climatological flux. The flux anomaly is held constant throughout the annual cycle. It is fluxed to the standard mask shown in figure 2 and distributed evenly in the upper 200 meters. A range of water masks are tested including East Antarctic, West Antarctic and masks the mimic climatological distribution of ice-bergs. Alterations to the mask were found to be relatively inconsequential for model results; therefore, the default ModelE mask is used to maintain simplicity.

Application of linear convolution theory

Linear Convolution Theory (Equation 1) is used to estimate the response of the model to any given meltwater scenario.

$$\widehat{SOSST}_{HistAMW}(t) \approx \sum_i \int_{t-\tau_{max}}^{t} SST_{StepAMW}(t-t',i) \frac{d\ AMW_{Hist}(t,i)}{dt}\bigg|_{t'} dt' \quad (1)$$

Where $SST_{StepAMW}$ is the SOSST response of modelE2.1 to a step change in forcing, AMW_{Hist} is a given meltwater scenario and $SOSST_{HistAMW}$ is the estimated SOSST response to the given scenario.

It is expected that the error of LCT projections will increase for extreme scenarios where AMW_{Hist} is much larger then the perturbation experiment. For example, initial experiments suggest that the scaled response of Southern Ocean SST to a 6000 Gt/yr step increase in meltwater is around a half of the response of the response to 200 Gt/yr.

References

Dee, D.P., Uppala, S.M., Simmons, A.J., Berrisford, P., Poli, P., Kobayashi, S., Andrae, U., Balmaseda, M.A., Balsamo, G., Bauer, D.P. and Bechtold, P., 2011. The ERA‐Interim reanalysis: Configuration and performance of the data assimilation system. *Quarterly Journal of the royal meteorological society*, *137*(656), pp.553-597.

Tournadre, J., Bouhier, N., Girard-Ardhuin, F. and Rémy, F., 2016. Antarctic icebergs distributions 1992–2014. *Journal of Geophysical Research: Oceans*, *121*(1), pp.327-349.